JOURNAL OF SOLID STATE CHEMISTRY 116, 378–384 (1995)

Relation between Valence Force Constants and Elastic Constants in α-Alumina: Evolution at High Temperatures

Y. Repelin,* E. Husson,†,[1] and C. Proust†

*Laboratoire de Chimie Physique du Solide, URA CNRS 453, Ecole Centrale de Paris, 92295 Chatenay-Malabry Cedex, France; and †Laboratoire de Physique et Mécanique des Matériaux, ESEM, Université d'Orléans et CRPHT-CNRS, 45071 Orléans Cedex 2, France

Received July 13, 1994; in revised form October 24, 1994; accepted November 16, 1994

A general valence force field is determined from the experimental vibrational frequencies and elastic constants of α-Al_2O_3 in order to relate the macroscopic elasticity of this material to its microscopic elasticity characterized by the bond-stretching and angle-bending force constants. The evolution of the frequencies, elastic constants, and force field as a function of temperature is discussed. © 1995 Academic Press, Inc.

INTRODUCTION

A general relation between force constants and elastic constants in a crystal was discussed by Born and Huang (1). Then Shiro and Miyazawa (2) developed a general matrix method, from the GF matrix method of Wilson *et al.* (3), for treating elastic constants from force fields of crystals. They showed that an identical GVFF may be used to calculate (i) the vibrational frequencies and (ii) the elastic constants of a molecular crystal with the application of polyethylene. Partial derivatives of elastic constants with respect to force constants were also calculated, for least-square adjustments of force fields with reference to experimental elastic constants as well as vibrational frequencies. This calculation makes it possible to know what are the internal coordinates (bond stretchings, bond angle bendings, torsions) which are concerned in a given vibrational frequency or a given elastic constant. If the GF matrix method was commonly used for treating the factor-group vibrations of crystal lattices and adjusting force constants sets with reference to observed infrared and Raman frequencies, very little has been published to our knowledge on the relation between force constants and elastic constants and authors did not discuss the internal coordinates concerned in the elastic constants.

The aim of our work is (i) to study the relation between force constants and elastic constants in different materials, (ii) to analyze the bonds and bond angles concerned in the compressive and shear constants in order to understand the macroscopic elastic behavior of these materials, and (iii) to evaluate if a rough prediction of the elastic constants of a material is possible from the force field obtained by vibrational spectroscopy data. To be valuable, the method should lead to using the smallest number of force constants as possible: principal force constants of stretching, bending, and torsion but also interaction constants such as stretching/stretching, stretching/bending, and bending/bending interactions. If the principal force constants of a compound may be approximated before calculations from force fields previously published for close compounds having the same type of chemical bonds, it is generally difficult to predict which interaction constants are the most important. And the more compact the crystal framework, the greater and the more numerous the interaction constants. For these reasons, the first material we studied was α-Al_2O_3 which exhibits a great compactness due to the face sharing of AlO_6 octahedra and to the high coordination of Al and O atoms respectively 6 and 4. Experimental Raman and IR spectra as well as elastic constants are known but no force field calculation was published for this compound.

In the second part of the work, the evolution of the frequencies, elastic constants, and force field constants as a function of temperature is discussed.

CALCULATION METHODS

The determination of GVFF force constants from the vibrational spectra is based on the Wilson *et al.* GF matrix method (3) extended to the crystal using the method given by Shimanouchi *et al.* (4). The programs used are the Schachtschneider GMAT and VSEC (5) applied to molecules or crystals and modified by Bates in order to extend the method to a tridimensional crystal (6).

The C_{ij} elastic tensor elements may be calculated from the force constants by the matricial method developed by Shiro and Miyazawa (2) from the Born and Huang theory (1). The elasticity tensor matrix is given by the general

---

[1] To whom correspondence should be addressed.

0022-4596/95 $6.00

formula

$$C = (\tilde{D}_\sigma F^\circ_R D_\sigma - \tilde{D}_\sigma F^\circ_R B_\rho [\tilde{B}_\rho F^\circ_R B_\rho]^{-1} \tilde{B}_\rho F^\circ_R D_\sigma)/V,$$

where F°_R is the potential energy matrix (force constants matrix), D is the dynamical matrix defined from the internal coordinate matrix and the atomic positions, B is the transformation matrix of cartesian coordinates into internal coordinates, and V is the crystal cell volume. The program written by the authors calculates also the partial derivatives of the elastic constants against the force constants (potential energy distribution or PED).

PREVIOUS STRUCTURAL VIBRATIONAL AND ELASTIC DATA ON α-ALUMINA

Structural Data

The crystal structure of α-Al_2O_3 or corundum has been determined by different authors (7–9). The space group is $R3c$ (D^6_{3d}) with cell parameters a_h = 0.4754 nm and c_h = 1.299 nm at 300 K. The rhombohedral cell contains two formular units. Al atoms lie on the C_3 axis (4c), whereas O atoms lie on C_2 axes (6e). O atoms occupy approximately hexagonal-close-packed positions with metal atoms occupying two-thirds of the octahedral interstices. In this structure distorted AlO_6 octahedra are linked by faces, edges, or corners in such a way that each O atom is linked to four Al atoms. The projection of the structure in the *bc* plane is given in Fig. 1. Two types of Al–O bonds exist in an AlO_6 octahedron: three Al–O bonds pointing toward the common face of two octahedra with a length of 0.1971 nm and three others of 0.1852 nm length.

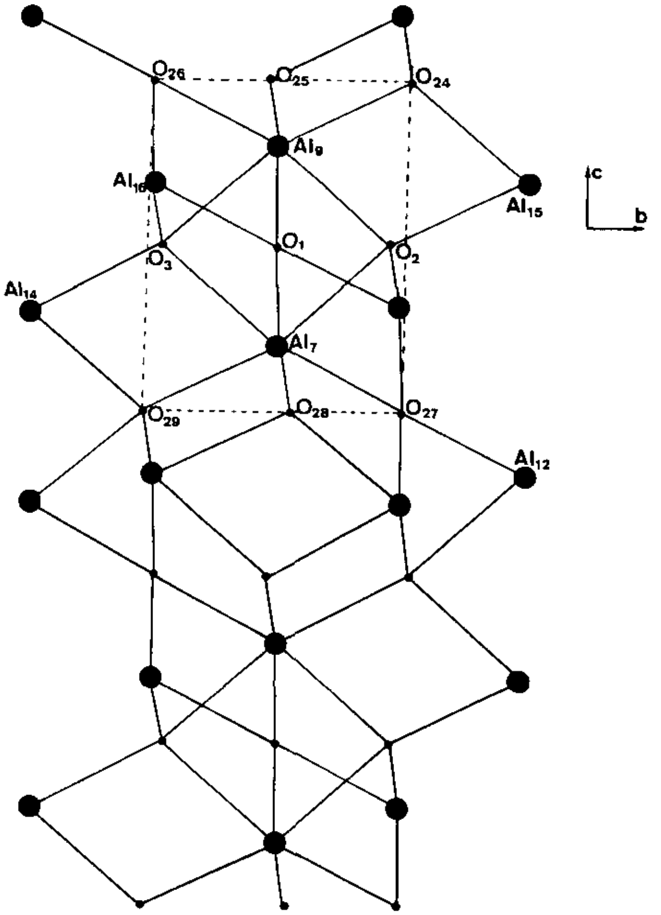

FIG. 1. Projection of the structure of α-Al_2O_3 in the *bc* plane (dashed lines indicate the unit cell).

TABLE 1

Interatomic Distances (nm), Bond Angles (°), and Cell Parameters with Their Standard Deviations in Parentheses at 300 and 2170 K and the Variation (%) in Comparison to the Values at 300 K

T	300 K	2170 K	Var (%)
d_1	0.1852(1)	0.1880(1)	+2.69
d_2	0.1971(2)	0.2024(2)	+1.51
δ_1	79.53(7)	79.09(9)	−0.55
$\delta_2 = \delta_3$	86.40(6)	86.42(9)	0
δ_4	101.20(5)	101.57(9)	+0.36
α_1	84.76(10)	85.35(13)	+0.70
$\alpha_2 = \alpha_2'$	93.61	93.58	0
α_3	132.19	131.93	−0.20
α_4	120.38	120.41	0
Al–Al (face)	0.2657(4)	0.2744(4)	+3.3
Al–Al (edge)	0.2789(1)	0.2847(1)	+2.08
Al–Al (corner)	0.3214(1)	0.3262(2)	+1.5
a_h	0.4754(1)	0.4844(2)	+1.9
c_h	1.299(2)	1.327(2)	+2.15

The structure was studied up to 2170 K by Ishizawa *et al.* (9) by X ray diffraction and by Aldebert and Traverse by neutron time of flight diffraction (10). Significant changes in the positional parameters of the Al atoms and slight changes in those of the O atoms were observed. The distorted hexagonal-close-packed plane of O atoms becomes more regular at 2170 K, and the Al atoms move toward the vacant octahedral interstices between the oxygen layers. The values of the cell parameters, bond lengths, and angles at 300 and 2170 K are reported in Table 1.

Spectroscopic Data

The irreducible representations for the optical and acoustical modes from the Bhagavantam and Venkataryudu method (11) are

$$\Gamma_{op} = \underset{(R)}{2A_{1g}} + \underset{(i)}{3A_{2g}} + \underset{(R)}{5E_g} + \underset{(i)}{2A_{1u}} + \underset{(IR)}{2A_{2u}} + \underset{(IR)}{4E_u}$$

$$\Gamma_{ac} = A_{2u} + E_u$$

The Raman and IR spectra have been published by different authors (12–18). Ashkin *et al.* (13) have shown the temperature dependence of some of the Raman lines and linewidths in the range of 77–1200 K; Richet *et al.* (14) studied the Raman spectra of Al_2O_3 up to 1800 K. Gervais *et al.* give the evolution of the IR frequencies up to 975 K for the A_{2u} modes (17) and up to 1775 K for the E_u modes (18).

Elastic Constants Data

The elastic constants of α-Al_2O_3 have been determined by some authors (19–21). The evolution of the C_{ij} was studied by Goto *et al.* (20) up to 1825 K and by Zouboulis and Grimsditch (21) up to 2100 K. In this work the Goto *et al.* C_{ij} values were chosen.

RESULTS AND DISCUSSION

Normal Coordinate Analysis at 300 K

The internal coordinate sets introduced in the normal coordinate analysis are presented in Table 2. There are two sets of Al–O bonds, the d_1 set corresponds to the bonds pointing toward the common face of octahedra and the d_2 set to the others; four sets of O–Al–O angles δ (with $\delta_2 \equiv \delta_3$); and five sets of Al–O–Al angles α (with $\alpha_2 \equiv \alpha_5$). On the whole 126 internal coordinates were introduced.

In order to obtain a better fit between the observed and calculated frequencies and elastic constants, it was necessary to add interaction constants. Different stretching/stretching (d/d), stretching/bending (d/α, d/δ), and bending/bending (α/α, δ/δ, δ/α) interactions were introduced and only those having significant values were kept in the final refinement. They are listed in Table 2.

The values of the force and interaction constants at 300 K are reported in Table 2; the comparison between observed and calculated frequencies, between observed and calculated elastic constants, and PED are given respectively in Tables 3 and 4.

The examination of the results shows that six principal constants and 11 interaction constants were introduced to fit together the vibrational frequencies and the C_{ij} elastic constants. For the vibrational frequencies fit, the average error is 2.3%, which is quite satisfactory. For the elastic constants the average error is about 6.2% for the principal constants C_{ii}; the C_{ij} terms which are generally less precise are more difficult to fit.

Identical force constants were fixed for the d_1 and d_2 bonds. Two of the authors (Y.R. and E.H.) showed that in structures containing MO_6 octahedra the most important parameters for the M–O stretching force constants are:

(i) The degree of bridging of oxygen atoms. The force constants decrease substantially as the oxygen atom coordinence increases.

(ii) The type of linkage of the octahedra. If they are isolated the M–O force constants are smaller than if they are linked; in a tridimensional MO_6 framework, the M–O bond constants increase when the octahedra are linked by corners, by edges, or by faces. Moreover, for a same type of bond, the smaller the bond length, the stronger the force constant (22).

In Al_2O_3 all the O atoms are linked to four Al atoms; the d_1 bonds pointing toward the common face of two

TABLE 2

Definition and Values of the Force Constants and Interaction Constants f Introduced in the Fits (Stretching and Stretching/Stretching in $N \cdot cm^{-1}$, Bending in $N \cdot cm \cdot rad^{-2}$, Stretching/Bending in $N \cdot rad^{-1}$)

Force constants				Interaction constants			
	Type	d (nm), α, δ(°)	f		Type		f
d_1	Al_7O_1	0.1971(2)	1,14	d_{11}	Al_7O_1/O_1Al_9	dd	0.08
d_2	Al_7O_{27}	0.1852(1)	1,14	d_{22}	$Al_7O_{27}/O_{27}Al_{12}$		0.08
δ_1	$O_1Al_7O_2$	79.53(7)	0.51	d'_{11}	O_1Al_7/Al_7O_2	dd'	0.10
δ_2	$O_2Al_9O_{25}$	86.40(6)	0.45	d'_{22}	$O_{24}Al_9/Al_9O_{25}$		0.10
δ_3	$O_3Al_7O_{29}$	86.40(6)	0.45	d_{11}	$Al_9O_1/Al_{16}O_{26}$		0.20
δ_4	$O_{24}Al_9O_{25}$	101.20(5)	0.45	d_{22}	$Al_9O_{24}/Al_{15}O_2$		0.26
α_1	$Al_7O_1Al_9$	84.76(10)	0.35	d^{+}_{11}	Al_7O_1/Al_9O_2		0.22
α_2	$Al_7O_3Al_{14}$	93.61(6)	0.23	d^{+}_{22}	$Al_9O_{24}/Al_{15}O_2$		0.26
α'_2	$Al_7O_{29}Al_{14}$	93.61(6)	0.23	d^{*}_{22}	Al_7O_{28}/Al_9O_{25}		0.22
α_3	$Al_7O_3Al_{16}$	132.19(3)	0.20	d_{12}	Al_7O_1/O_1Al_{16}		0.20
α_4	$Al_7O_{27}Al_{12}$	120.38(4)	0.20	d'_{12}	O_1Al_7/Al_7O_{27}		0.26
				d'''_{12}	O_1Al_7/Al_7O_{29}		0.26
				d''_{12}	O_1Al_7/Al_7O_{28}		−0.10
				$d\delta_1$	$Al_7O_{29}/O_{27}Al_7O_{28}$		0.05
				$d\delta_2$	$Al_7O_1/O_{27}Al_7O_{29}$		0.05

TABLE 3
Observed and Calculated Frequencies and PED in α-Al_2O_3

	ν (cm^{-1})		
Mode	Experimental	Calculated	PED[a]
E_g	750	729.1	$16d_1 + 42d_2 + 12d'_{12} + 13d^{+}_{22}$
A_g	644	646.3	$55d_1 + 25d_2 + 14dd' - 26d_{12} + 19d_{11} - 17d'_{12} - 17d'''_{12} + 18d^{+}_{22}$
E_u	634	649.3	$27d_1 + 43d_2 + 12\delta_2 + 20\alpha - 15d'''_{12} - 16d^{+}_{22}$
A_{2u}	584	583.1	$60d_1 + 37d_2 + 19\delta_1 + 17\delta_3 + 12\alpha_2 + 12\alpha_5 + 17dd' - 21d_{11} - 21d'_{12} + 9d''_{12} - 21d'''_{12} - 22d^{+}_{22}$
E_g	576	563.4	$31d_1 + 20d_2 + 19\delta + 12d_{12} + 12d^{+}_{22}$
E_u	569.5	540.8	$27d_1 + 36d_2 + 12\delta_1 + 12\delta_{1,4} + 20\alpha - 14d^{+}_{22}$
E_g	448	468.2	$15\delta_1 + 17\delta_3 + 19\delta_4 + 45\alpha_2 \rightarrow {}_5$
E_u	439,3	448.3	$82d_1 + 27d_2 + 28\delta + 13d_{11} - 20d'''_{12} - 25d^{+}_{22}$
E_g	428	430.8	$58d_1 + 60d_2 + 27\delta + 18\alpha - 35d_{12} - 20d'_{12} - 12d^{*}_{22} + 27d^{+}_{22}$
A_g	416	400.8	$38\delta_1 + 17\delta_4 + 22\alpha_1 + 17\alpha_4$
A_{2u}	399,5	384.3	$68d_2 + 17\delta + 24\alpha_3 + 13dd' - 13d^{*}_{22} - 16d^{+}_{22}$
E_u	384,8	378.2	$50d_2 + 30\delta_2 + 17\delta_3 + 17\alpha_{2\rightarrow5} - 12d^{+}_{22}$
E_g	378	375.6	$45d_1 + 16\delta_2 + 14\alpha_3 + 13\alpha$

[a] Only the contributions ≥ 12% are mentioned.

octahedra are supposed to be stronger than the d_2 bonds (edge-linked octahedra) but d_1 bonds are longer than d_2 bonds. Thus the two types of bonds are expected to have close force constants. The value 1.14 N · cm^{-1} can be compared with those found (about 1.10 N · cm^{-1}) in perovskites $EuAlO_3$ and $NdAlO_3$ (23, 24). In these compounds the Al–O bonds exhibit a length of 0.190 nm and each oxygen atom is linked to two Al atoms instead of four in Al_2O_3, whereas octahedra share only corners instead of corners, edges, and faces in Al_2O_3. With the two parameters playing in opposite sense, it seems coherent to have force constants of about the same value for the two structures.

For the O–Al–O angles the bending force constants are 0.51 N · cm^{-1} for δ_1 which is the angle between two d_1 bonds and they are smaller, 0.45 N · cm^{-1}, for the others. For the Al–O–Al angles again the bending force constant applying to the α_1 angle is higher than in the other α angles. Concerning the interaction constants the strongest are the AlO/AlO ones with a common Al or O atom but also those between Al–O bonds belonging to two different AlO_6 octahedra with no common atom, for example $f(d^{+}_{11})$ between d_1 bonds joined via the common face or $f(d^{*}_{22})$ between d_2 bonds in a $\mathrm{Al}{<}^{\mathrm{O}}_{\mathrm{O}}{>}\mathrm{Al}$ cycle (in edge-sharing octahedra). The stretching/bending and bending/bending interactions are negligible except for the two constants $fd\delta_1$ and $fd\delta_2$ which exhibit a low value (0.05 N · cm^{-1}).

The examination of Table 3 reveals the following results:

— For the highest frequencies due essentially to stretching modes, there is an important coupling between the stretching vibrations of the d_1 and d_2 bonds. This is due to the compacity of the structure and confirms that the two sets of bonds vibrate together and thus have close force constants.

— The bending modes appear at relatively high frequencies coupled with the stretching modes.

TABLE 4
Observed and Calculated Elastic Constants and PED in α-Al_2O_3

	(GPa)		
C_{ij}	Experimental	Calculated	PED[a]
C_{11}	497	492	$38d_2 + 23\delta + 13\alpha$
C_{33}	500,9	428.4	$24d_2 + 35\delta + 14\alpha$
C_{44}	146,8	146	$16d_1 + 53d_2 + 25\delta_{2\rightarrow4} + 15\alpha$
C_{66}	167,5	153	$16d_2 + 48\delta + 19\alpha$
C_{12}	164	185.6	$97d_2 - 10\delta_1 - 20\delta_2 - 18\delta_3 - 18\alpha + 16dd' + 15d_{12}$
C_{13}	116	201.7	$15d_1 + 89d_2 - 22\delta - 20\alpha + 12d^{+}_{22} + 12d\delta$
C_{15}	−21,9	−6.6	$-44d_1 + 31d_2 - 20\alpha - 13dd + 24dd' + 54d_{12} + 24d'_{12} + 20d''_{12} + 24d'''_{12}$

[a] Only the contributions ≥ 12% are mentioned.

— The Al–O–Al angle bending notably contributes to the PED, as does the O–Al–O angle bending.

From Table 4 it can be concluded that:

- Compressibility constants C_{11} and C_{33} are both due to Al–O bonds and to O–Al–O and Al–O–Al angles. Although all δ and α angle sets are concerned, only d_2 bonds are.

— For the C_{44} shear constant there is a predominant contribution of the d_2 bonds, the δ angles except δ_1, the α angles except α_1, and the d_1 bonds. For the C_{66} constant an important contribution of the angles and more particularly of δ angles is noted.

— Thus both the d_1 bonds pointing toward the common face of two octahedra and the corresponding δ_1 and α_1 angles which constitute the most rigid part of the crystal exhibit a low contribution to the C_{ii} elastic constants.

— The C_{ij} terms exhibit a predominant contribution of the Al–O bonds.

Evolution as a Function of Temperature

In Fig. 2 the evolution of the Raman (14) and IR frequencies (17, 18) vs temperature have been reported. All the frequencies decrease linearly when the temperature increases. Figure 3 gives the temperature variation of elastic constants according to Goto *et al.* (20). The C_{11}, C_{33}, and C_{44} constants decrease linearly with temperature, whereas the C_{12}, C_{13}, and C_{14} constants remain quite constant in the whole temperature range.

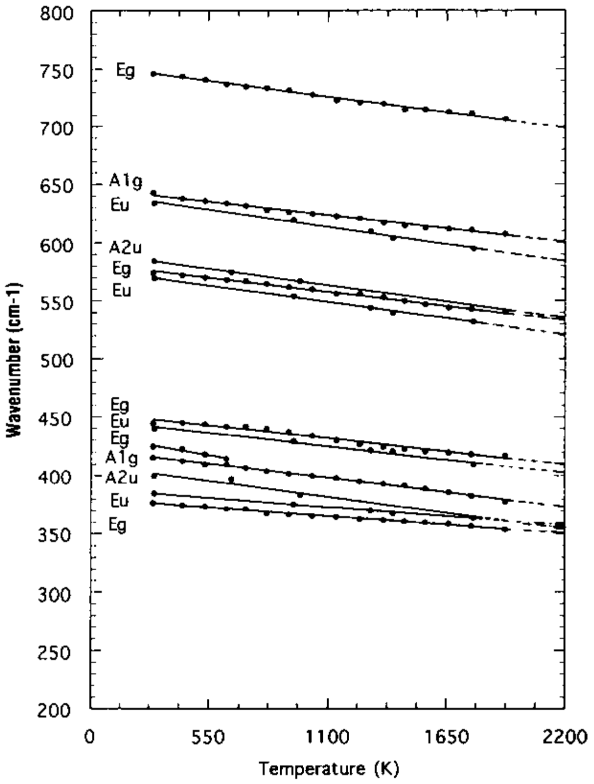

FIG. 2. Evolution of the Raman and IR frequencies vs temperature (14, 17, 18).

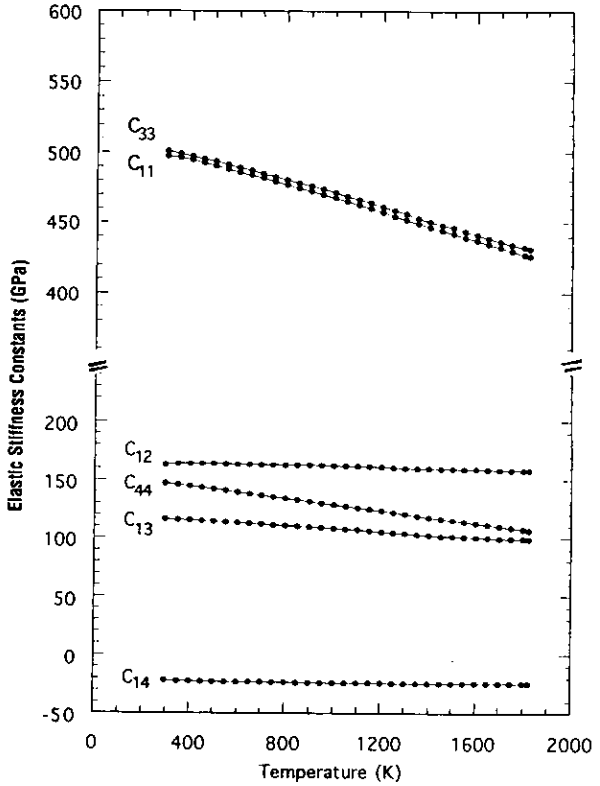

FIG. 3. Evolution of the elastic constants vs temperature according to Goto *et al.* (20).

Fits have been made for the data at 620, 1450, 1770, and 2170 K. For the highest temperatures, spectroscopic data were extrapolated from the curves of Fig. 2 and experimental C_{ij} of Zouboulis and Grimsditch were used. For the last temperature, two calculations were performed: (i) with the atomic positions at 300 K and (ii) with the atomic positions determined by Ishizawa *et al.* at 2170 K (9). The interaction constants calculated at 300 K were kept constant in the calculations at higher temperatures and only the principal force constants were adjusted. The observed and calculated frequencies and elastic constants are given respectively in Tables 5 and 6 and the force constants are given in Table 7.

The examination of the results makes possible the following remarks:

— It was possible to transfer the force field determined at 300 K to fit the experimental data at higher temperatures. The different fits between the observed and calculated data lead to an average error of 2.3% for the vibrational frequencies and 7% for the elastic C_{ii} constants. The PED remains quite identical except for C_{44} where the contribution of the d_2 bonds increases regularly from 58% at 300 K to 72% at 2170 K.

TABLE 5

Observed and Calculated Frequencies (in cm^{-1}) at Different Temperatures

	620		1450		1770		2170		
T(K)	Observed	Calculated	Observed	Calculated	Observed	Calculated	Observed	Calculated[a]	Calculated[b]
E_g	738	726.9	714	714.1	710	700.4	692	691.2	688.9
A_g	634	644.9	615	632.6	610	617.4	605	607.5	606.3
E_u	625	643.1	604	617	595	598	584	586.1	575.8
A_{2u}	574.5	577.6	560	560.2	545	538.7	540	522.2	514.3
E_g	568	562.1	548	549.6	543	539.3	530	531.8	526.1
E_u	560	535.7	540	517.2	532	502.5	522	492.6	485.7
E_g	442	459.0	430	442.0	420	433.4	410	427.9	416.7
E_u	432	446.4	421	431.4	410	414.4	402	401.7	396.7
E_g	416	428.8	386	410.3	376	392.7	366	380.9	376.3
A_g	409	394.1	386	377.5	376	370	364	365.8	359.1
A_{2u}	392.5	379.2	380	365.6	365	354.1	352	347.3	343.5
E_u	380	375.8	365	359.6	364	350.5	358	343.7	339.1
E_g	373	371.2	357.5	358.5	352	348.7	345	342.1	338.5

[a] Calculations performed with the atomic positions at 300 K.
[b] Calculations performed with the atomic positions at 2170 K.

— Between 300 and 2170 K the force constants decrease about 12% for the Al–O bonds, 14% for the O–Al–O angles, and 20% for the Al–O–Al angles.

— All the vibrational frequencies exhibit a very similar evolution between 300 and 2170 K, due to the important couplings between stretching and bending modes. This result is in good agreement with those of Schauer (25) who observed an average 4.1% decrease of the frequencies between 300 and 1470 K. Comparing the frequencies at 2170 K with those at 300 K, one can note a lesser decrease of high frequencies exhibiting a predominant contribution of the stretching modes. The frequencies E_g at 448.7 cm^{-1} and A_g at 417.4 cm^{-1} due only to bending modes exhibit a greater decrease.

— For the elastic constants a very important decrease of compressibility constants C_{11} and C_{33} can be observed in Fig. 3; C_{44} exhibits a lower decrease and C_{12}, C_{13}, and C_{14} remain quite constant. It seems that the greater contribution Al–O bonds exhibit, the lesser variation they show with the temperature.

CONCLUSION

This work gives the following main results:

(i) It was possible with a limited number of force and interaction constants to fit the vibrational frequencies and the elastic constants with a satisfactory precision in α-Al_2O_3.

(ii) The importance of the interaction constants was pointed out, especially stretching/stretching interactions. This is related to the great compacity of the structure and the high coordination of oxygen atoms.

(iii) The bonds and angles assumed to be the most rigid do not occur in the elastic constants, especially in the compressibility constants which are high: α-Al_2O_3 is one

TABLE 6

Observed and Calculated Elastic Constants (in GPa) at Different Temperatures

	620		1450		1770		2170	
T(K)	Observed	Calculated	Observed	Calculated	Observed	Calculated	Observed[a]	Calculated
C_{11}	483.8	487.1	444.3	465.3	429.6	453.6	405	444
C_{33}	487.2	425.6	448.3	403.1	434.5	396.2	413	387.9
C_{44}	137.9	144.2	116.3	132.6	108.7	125.8	100	120
C_{66}	160.3	149.5	142.5	136.8	135.7	132.9		129.5
C_{12}	163.1	188.1	159.2	191.7	158.1	187.8		185.1
C_{13}	112.5	203	101.6	206.4	99.2	199.7		197.2
C_{14}	−23.4	−6.2	−24.5	−7.5	−24.5	−6.5		−7.2

[a] Experimental data of Zouboulis and Grimsditch (21).

TABLE 7
Evolution of the Principal Force Constants vs Temperature (Stretching in $N \cdot cm^{-1}$, Bending in $N \cdot cm \cdot rad^{-2}$)

T(K)	300	620	1450	1770	2170[a]	Var(%)[b]
$d_1 = d_2$	1.14	1.14	1.10	1.04	1.00	−12
δ_1	0.51	0.49	0.48	0.47	0.46	−10
$\delta_2 = \delta_3 = \delta_4$	0.45	0.45	0.40	0.39	0.38	−15
α_1	0.35	0.35	0.30	0.28	0.27	−23
$\alpha_2 = \alpha'_2$	0.23	0.22	0.22	0.21	0.20	−13
$\alpha_3 = \alpha_4$	0.20	0.18	0.16	0.15	0.15	−25

[a] Force field used for the fits performed with the atomic positions at 2170 and 300 K.

[b] Variation between the values at 2170 and 300 K.

of the most incompressible materials, with a bulk modulus of 252 GPa (26).

(iv) When the temperature increases, the structure exhibits very slight evolution, leading to slight evolution of the vibrational frequencies and elastic constants since the bulk modulus decreases from 252 GPa at 300 K to 221 GPa at 1825 K (26, 27).

(v) The stretching force constant decreases slowly from 1.14 $N \cdot cm^{-1}$ at 300 K to 1.04 $N \cdot cm^{-1}$ at 2170 K. Thus the Al–O bonds are fairly weakened at high temperature. They kept approximately the same degree of covalency at high temperature as at 300 K. This result is in good agreement with the slight evolution vs temperature of the Gruneisen parameters given by Schauer (25): 1.40 at 300 K and 1.32 at 1475 K. The bending constants, especially the Al–O–Al ones, weaken more with increasing temperature.

REFERENCES

1. M. Born and K. Huang, "Dynamical Theory of Crystal Lattices." Oxford Univ. Press, London, 1954.
2. Y. Shiro and T. Miyazawa, *Bull. Chem. Soc. Jpn.* **44,** 2371 (1971).
3. E. B. Wilson, J. C. Decius, and P. C. Cross, "Molecular Vibrations, the Theory of Infrared and Raman Vibrational Spectra." McGraw–Hill, New York, 1955.
4. T. Shimanouchi, M. Tsuboï, and T. Miyazawa, *J. Chem. Phys.* **35,** 1597 (1961).
5. J. H. Schachtschneider, Shell Development Co. Technical Report 231 (1964).
6. J. B. Bates, *J. Chem. Phys.* **56,** 1910 (1972).
7. L. Pauling and S. B. Hendricks, *J. Am. Ceram. Soc.* **47,** 781 (1925).
8. R. E. Newnham and Y. M. de Haan, *Z. Kristallogr.* **117,** 235 (1962).
9. N. Ishizawa, T. Miyata, I. Minato, F. Marumo, and S. Iwai, *Acta Crystallogr. Sect. B* **36,** 228 (1980).
10. P. Aldebert and J. P. Traverse, *High Temp. High Pressures* **16,** 127 (1984).
11. S. Bhagavantam and T. Venkataryudu, *Proc. Indian Acad. Sci. Part A* **9,** 224 (1939).
12. S. P. S Porto and R. S. Krishnan, *J. Chem. Phys.* **47,** 1009 (1967).
13. M. Ashkin, J. H. Parker, Jr., and D. W. Feldman, *Solid State Commun.* **6,** 343 (1968).
14. P. Richet, P. Gillet, A. Pierre, M. Ali Bouhifd, I. Daniel, and G. Fiquet, *J. Appl. Phys.* **74,** 5451 (1993).
15. G. H. Watson, Jr., W. B. Daniels, and C. S. Wang, *J. Appl. Phys.* **52,** 956 (1981).
16. A. S. Barker, Jr., *Phys. Rev.* **132,** 1474 (1963).
17. F. Gervais and B. Piriou, *J. Phys. C: Solid State Phys.* **7,** 2374 (1974).
18. F. Gervais, D. Billard and B. Piriou, *Rev. Int. Hautes Temp. Réfract.* **12,** 58 (1975).
19. J. H. Gieske and G. R. Barsch, *Phys. Status Solidi* **29,** 121 (1968).
20. T. Goto, O. L. Anderson, I. Ohno, and S. Yamamoto, *J. Geophys. Res.* **94,** 7588 (1989).
21. E. S. Zouboulis and M. Grimsditch, *J. Appl. Phys.* **70,** 772 (1991).
22. E. Husson and Y. Repelin, *C. R. Acad. Sc. Paris Sér. II* **296,** 1405 (1983).
23. M. C. Saine, E. Husson, H. Brusset, and A. Cerez, *Spectrochim. Acta Part A* **37,** 985 (1981).
24. M. C. Saine and E. Husson, *Spectrochim. Acta Part A* **40,** 733, (1984).
25. A. Schauer, *Can. J. Phys.* **43,** 523 (1965).
26. E. Schreiber and O. L. Anderson, *J. Am. Ceram. Soc.* **49,** 184 (1965).
27. O. L. Anderson, *J. Phys. Chem. Solids* **27,** 547 (1966).